Photoelectrochemical Cells Based on Amorphous Hydrogenated Silicon Thin Film Electrodes and the Behavior of Photoconductor Electrode Materials

Gary S. Calabrese,[1] Mou-Shiung Lin,[1] Joseph Dresner,[2] and Mark S. Wrighton*[1]

Contribution from the Department of Chemistry, Massachusetts Institute of Technology, Cambridge, Massachusetts 02139, and the RCA Laboratories, David Sarnoff Research Center, Princeton, New Jersey 08540. *Received September 14, 1981*

Abstract: The behavior of intrinsic a-Si:H photoanodes has been investigated. Thin films (~3.9 μm) of intrinsic a-Si:H, on a stainless steel substrate coated with a very thin (~200 Å) heavily n-type doped a-Si:H layer for ohmic contacting, behave as electrodes only under $\geq E_g$ = 1.7 eV illumination, irrespective of the $E^{\circ\prime}$ of the redox couple investigated in the range −1.78 to +0.41 V vs. SCE in CH_3CN/0.1 M [n-Bu_4N]ClO_4. The nature of the contact, stainless steel/n-type a-Si:H/intrinsic a-Si:H, indicates that redox couples having $E^{\circ\prime}$ more positive than the bottom of the conduction band, E_{CB}, can result in a field across the intrinsic a-Si:H that will drive photogenerated holes to the surface in contact with the redox couple while the electrons excited to the conduction band are driven into the bulk. Electrochemical measurements establish the E_{CB} position in EtOH/ or CH_3CN/0.1 M [n-Bu_4N]ClO_4 to be at ~−0.7 ± 0.1 V vs. SCE. For $E^{\circ\prime}$ more negative than −0.7 V vs. SCE, fast, one-electron, outer-sphere redox couples at ~1 mM concentration respond to the illuminated a-Si:H as they do at Pt. For $E^{\circ\prime}$ more positive than −0.7 V vs. SCE, the oxidation of the reduced form of the redox couple can occur at a more negative position than at Pt. In cyclic voltammetry experiments, the extent to which the oxidation peak is more negative than at Pt is a measure of the photovoltage, E_V, that could be obtained at open circuit in the presence of equal concentrations of the oxidized and reduced forms of the couple. Surface photocorrosion of a-Si:H is a problem at low (~1 mM) concentrations of redox reagents used in cyclic voltammetry, and the largest E_V found is ~0.4 V at ~40 mW/cm² of 632.8-nm light. Derivatization of a-Si:H with (1,1′-ferrocenediyl)dichlorosilane suppresses photocorrosion, and E_V of ~0.75 V has been obtained for this surface-confined ferrocene derivative, exceeding the E_V on single-crystal n-type Si photoanodes. Durable cells using a Pt cathode, the a-Si:H photoanode, and a EtOH/0.1 M [n-Bu_4N]ClO_4/10^{-3} M ferricenium/0.07 M ferrocene solution have been studied. The E_V seen is up to 0.75 V at 9.3 mW/cm² of 632.8-nm light. Constant output for ~100 h has been observed with an optimum efficiency of ~4.5% for conversion of 0.7 mW/cm² 632.8-nm light to electricity. This overall efficiency is slightly larger than that obtained for similar cells based on single-crystal n-type Si photoanodes.

Amorphous hydrogenated silicon, a-Si:H, is a material of interest in photovoltaic devices inasmuch as it is prepared from abundant elements, is synthesized as a genuine thin film, and has a wavelength response that is close to the optimum for solar energy conversion.[3] One kind of photovoltaic device[4] that can be envisioned is one where a photoconductor is sandwiched between two different metals having different work functions, ϕ (Scheme I).[5] In such a device the maximum possible photovoltage, E_V, that can be realized is the difference between ϕ_1 and ϕ_2 for M_1 and M_2, respectively, or the separation of the valence and conduction band, E_g, whichever is smaller.[4,5] In practice the objective is to contact the photoconductor at the bottom of the conduction band with one metal and at the top of the valence band with the other metal, as illustrated in Scheme I, since the position of the contacts will control whether the maximum possible E_V can actually be obtained. The field in the photoconductor separates the photogenerated carriers as illustrated. Carrier recombination rates and mobilities are among the important factors influencing the efficiency of such a device.

In this article, we report a study of the behavior of a-Si:H on stainless steel as an electrode material in an electrochemical cell. Such a cell is also a kind of photovoltaic device of the sort illustrated in Scheme I except that M_2 is replaced by a liquid electrolyte solution containing redox active material A^+/A with an associated electrochemical potential, $E_{redox}(A^+/A)$, that is the Fermi level. A representation of the energetics for a cell under illumination is given in Scheme II where we take the counterelectrode to be a material that is reversible for the A^+/A redox couple so that its electrochemical potential, E_f', is always that of the solution.

Scheme I. Representation of the Energetics for a Photovoltaic Device Consisting of a Photoconductor Sandwiched between Two Metals of Different Work Function

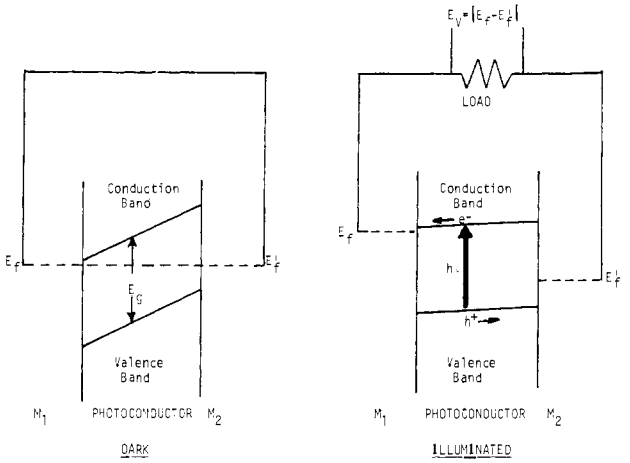

The key difference between the solid-state device represented by Scheme I and the photoelectrochemical device in Scheme II is that for the photoelectrochemical case there is an interface between the photoconductor and an ionic conductor. This means, of course, that when current flows redox reaction must occur at the photoconductor/liquid electrolyte interface, resulting in the oxidation of A to A^+. The behavior of electrode materials that exhibit significant conductivity only under illumination has not been examined extensively, though the behavior of semiconductor electrode materials has received a great deal of attention recently in connection with photoelectrochemical cells. The distinctions between photoconductors and semiconductors and metals will be illustrated by our results.

An a priori difference between a photoconductor electrode and a semiconductor is that the intrinsic photoconductor is capable of being either a photoanode *or* a photocathode depending on the

(1) Massachusetts Institute of Technology.
(2) RCA Laboratories, David Sarnoff Research Center.
(3) (a) Carlson, D. E.; Wronski, C. R.; Pankove, J. I.; Zanzucchi, P. J.; Staebler, D. L. *RCA Rev.* **1977**, *38*, 211. (b) Fritzche, H.; Tsai, C. C.; Persans, P. *Solid State Technol.* **1978**, *21*, 55.
(4) Rose, A. *Phys. Status Solidi A* **1979**, *56*, 11.
(5) Sze, S. M. "Physics of Semiconductor Devices"; Wiley: New York, 1969; Chapter 9.

0002-7863/82/1504-2412$01.25/0

Scheme II. Representation of the Energetics for a Photoelectrochemical Device Based on a Photoconductor as the Light Absorber

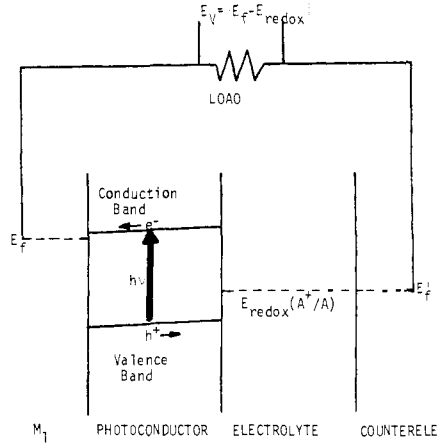

Scheme III. Representation of the Interface Energetics for a Photoconductor That Is a Photocathode[a]

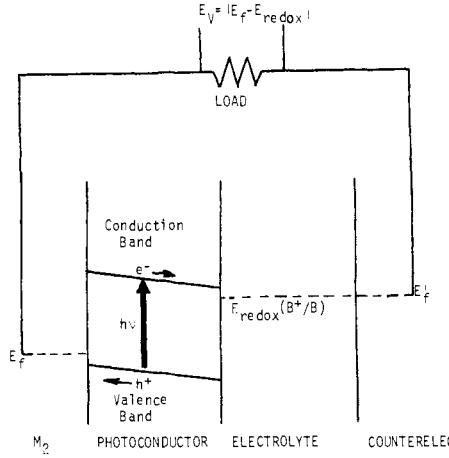

[a] In this case the metal M_2 contacts the valence band and not the conduction band as M_1 in Scheme II that results in a photoanode.

nature of the contacting metal. A semiconductor is a good photoanode if it is doped n-type or a good photocathode if it is doped p-type.[6] To see how the photoconductor can be changed from a photoanode to a photocathode, consider Schemes I and II. Notice that the Fermi level of M_1 contacts the photoconductor near the conduction band while M_2 contacts the photoconductor near the valence band leading to a field in the semiconductor such that excited electrons, e^-, go toward M_1 while the h^+'s go toward M_2. Thus, employing M_1 as the back metal results in a device where the field is such that photogenerated h^+'s go toward the electrode/liquid electrolyte interface while e^-'s are driven toward the M_1 contact. Since h^+'s go toward the interface, thermodynamically uphill oxidation processes can be effected when E_{redox} is sufficiently positive and the electrode is said to be a photoanode. To prepare a photocathode using the same photoconductor would involve changing the back metal to M_2, a metal that contacts the photoconductor near the valence band so that E_{redox} sufficiently negative gives a field in the photoconductor where e^-'s are driven to the electrode/liquid electrolyte interface to effect an uphill reduction (Scheme III). These a priori considerations illustrate the importance of knowing where the photoconductor is contacted by the E_{redox} of the solution and by the back metal.

A given photoconductor with a back metal M_3 can give uphill reductions or oxidations depending on the position of E_{redox}. If we take the Fermi level of M_3 to contact the photoconductor midway between the bottom of the conduction band and top of the valence band (Scheme IV), then the direction of the field will depend on whether E_{redox} is closer to the valence band or to the conduction band. In energy conversion applications, it is desirable to contact the semiconductor near one band or the other, since the field across the photoconductor can be the greatest under such circumstances.

Scheme IV. Representation of the Effect from E_{redox} Variation on Field Direction in a Photoconductor Contacted by a Metal M_3 That Contacts the Photoconductor Midway between the Conduction Band and the Valence Band

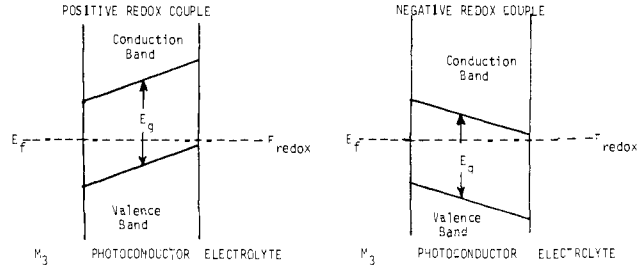

The chemistry at the interfaces between the contact metal and the photoconductor and between the photoconductor and the liquid electrolyte solution will control the field properties in the photoconductor. The difficulty of making predictions concerning semiconductor/metal, semiconductor/insulator, and semiconductor/liquid interfaces will undoubtedly be equally great for the photoconductor/liquid electrolyte interface.[7] Our study includes a characterization of the interface energetics of an a-Si:H photoconducting electrode in contact with a number of redox active materials.

A recent report on the use of a-Si:H as an electrode concerns the use of the material doped to be an n-type semiconductor. Disappointing results were obtained with respect to durability of the photosensitive surface and the value of E_V obtained.[8] Another report shows intrinsic a-Si:H to give excellent photovoltages in aqueous solutions, but again durability was lacking.[9] We show that essentially intrinsic a-Si:H can be used as a photoanode under illumination, and under certain conditions the material can be used to sustain conversion of light to electricity with respectable efficiency. The lack of durability of nonoxide photoanode materials is one of the major problems of photoelectrochemical cells, since the photogenerated hole, h^+, that comes to the electrode/electrolyte interface is capable, thermodynamically, of leading to the oxidation of the electrode.[10] The various ways of suppressing photoanodic decomposition[6,11] of semiconductors should apply to photoconductors as well, but it should be appreciated that while certain guidelines are emerging regarding suppression of electrode photocorrosion, each material has unique surface chemistry that may frustrate efforts to exploit the photovoltaic effect.

Experimental Section

Preparation of a-Si:H Electrode Material. The sample was prepared by the decomposition of SiH_4 in a DC glow discharge. The polished stainless steel substrate (anode) was held at T_s = 250 °C; the decomposition rate was 350 Å/min. A layer of n-type material (doped with 4.4% PH_3) 200 Å thick was deposited first in order to make ohmic contact to the substrate; this was followed by 3.9 μm of undoped a-SiH.

(6) Wrighton, M. S. *Acc. Chem. Res.* **1979**, *12*, 303.

(7) (a) Bard, A. J.; Bocarsly, A. B.; Fan, F.-R. F.; Walton, E. G.; Wrighton, M. S. *J. Am. Chem. Soc.* **1980**, *102*, 3671. (b) McGill, T. C. *J. Vac. Sci. Technol.* **1974**, *11*, 935. (c) Mead, C. A.; Spitzer, W. G. *Phys. Rev. [Sect.] A* **1964**, *134*, 713; (d) Mead, C. A.; Spitzer, W. G. *J. Appl. Phys.* **1963**, *34*, 3061.

(8) Avigal, Y.; Cahen, D.; Hodes, G.; Manassen, J.; Vainas, B.; Gibson, R. A. G. *J. Electrochem. Soc.* **1980**, *127*, 1209.

(9) Williams, R. *J. Appl. Phys.* **1979**, *50*, 2848.

(10) (a) Bard, A. J.; Wrighton, M. S. *J. Electrochem. Soc.* **1977**, *124*, 1706. (b) Gerischer, H. *J. Electroanal. Chem. Interfacial Electrochem.* **1977**, *82*, 133. (c) Park, S.-M.; Barber, M. E. *Ibid.* **1979**, *99*, 67.

(11) (a) Ellis, A. B.; Kaiser, S. W.; Wrighton, M. S. *J. Am. Chem. Soc.* **1976**, *98*, 1635. (b) Heller, A. *Acc. Chem. Res.* **1981**, *14*, 154. (c) Wrighton, M. S.; Bocarsly, A. B.; Bolts, J. M.; Bradley, M. G.; Fischer, A. B.; Lewis, N. S.; Palazzotto, M. C.; Walton, E. G. *Adv. Chem. Ser.* **1979**, *No. 184*, 269. (d) Noufi, R.; Frank, A. J.; Nozik, A. J. *J. Am. Chem. Soc.* **1981**, *103*, 1849. (e) Noufi, R.; Tench, D.; Warren, L. F. *J. Electrochem. Soc.* **1980**, *127*, 2310.

Analysis by SIMS showed the film to contain 15% H, 0.25% O, 250 ppm N, ~100 ppm C, and 25 ppm S. The optical band gap was found to be E_g = 1.70 eV. Undoped films of a-Si:H contain a small excess of donors of undetermined origin and are thus slightly n-type; the dark conductivity of similar samples at room temperature has been found to be in the range 10^{-8}–10^{-10} $(\Omega\ cm)^{-1}$. The minority carrier diffusion length, L_p, which is a sensitive index of material quality, was measured by the surface photovoltage method.[12] It varied along the surface of the samples from L_p = 0.3 to 1.0 μm under a background illumination of 10^{17} photons/(cm^2 s); from these values one obtains for holes $(\mu\tau)_p = 3.6 \times 10^{-8}$ to 4×10^{-7} $cm^2\ V^{-1}$.

Chemicals. HPLC grade CH_3CN was distilled from P_2O_5; [*n*-Bu_4N]ClO_4 (Southwestern Analytical Chemicals) was vacuum-dried at 70 °C for 24 h. The redox reagents used were commercially available or have been synthesized and used previously in related studies.

Equipment and Procedures. Cyclic voltammograms were recorded in Ar- or N_2-purged EtOH/ or CH_3CN/0.1 M [*n*-Bu_4N]ClO_4 solutions with redox reagents present at ~1 mM by use of a PAR Model 173 potentiostat controlled by a PAR Model 175 programmer. Scans were recorded with a Houston Instrument Model 2000 X-Y recorder. A single compartment, three-electrode cell was used with a Pt counterelectrode and either a saturated calomel reference electrode (SCE) or a silver wire (Ag/Ag^+) immersed in 0.1 M $AgNO_3$/0.1 M [*n*-Bu_4N]ClO_4 in CH_3CN (+0.35 V vs. SCE). Current vs. time plots were recorded on a Hewlett-Packard 7133A strip chart recorder. Electrodes were illuminated by using a beam-expanded 632.8 nm He–Ne laser (Aerotech) providing ~40 mW/cm^2. Laser intensity was varied by using a polarizing filter and was monitored with a beam splitter and a Tektronix J16 radiometer equipped with a J6502 probe. The laser beam was masked to match the size of the a-Si:H surface.

Electrode Preparation. The ~0.1 cm^2 a-Si:H samples were secured to coiled Cu wire with conducting silver epoxy by contact to the back (stainless steel) of the samples. The Cu wire lead was passed through a 4-mm glass tube, and then all surfaces were sealed with ordinary epoxy so as to leave only the front surface (a-Si:H) exposed.

Just prior to use, all electrodes were pretreated by etching at 25 °C in concentrated HF for 30 s, rinsed with distilled water followed by acetone, and air-dried.

Results and Discussion

a. Nature of the a-Si:H. The a-Si:H electrode material used in this study is essentially intrinsic material such that the Fermi level is situated about ~0.8 eV below the bottom of the conduction band when there is no field across the material. The contact to the stainless steel is via a very thin layer (~200 Å) of heavily doped n-type a-Si:H so that the representation in Scheme II adequately describes the situation: the nature of the back contact indicates that the electrode should serve as a photoanode capable of giving an output photovoltage, E_V, of up to $E_g \approx 1.7$ eV.

b. Behavior of Redox Couples at a-Si:H Electrodes. In order to explore the interface energetics and electron transfer kinetics, we have used nonaqueous electrolyte solutions containing various redox couples known to have fast heterogeneous electron-transfer kinetics at conventional electrode materials. Further, the redox materials used are all outer-sphere reagents that tend to preclude strong surface interactions that can alter the interface energetics.[13] Nonaqueous media have been used because deterioration of the electrode may be less important in the potential range of interest.[14] Thus, we believe that the interface energetics can be established by examining the redox behavior of solution reagents of variable formal potential, $E^{\circ\prime}$, as has been done for both p- and n-type semiconductor electrodes.[14,15]

A major difference between intrinsic a-Si:H and conventional electrodes or semiconductor electrodes is that the material has no significant conductivity in the dark. This means that any redox couple, independent of $E^{\circ\prime}$, will not respond to potential variation unless the material is exposed to illumination that creates charge carriers. Accordingly, the use of intrinsic a-Si:H as an electrode for any redox couple will require light of ≥1.7 eV at an intensity sufficient to achieve conductivity. Whether oxidation of the reduced form of a redox couple can be driven in an uphill sense depends on the $E^{\circ\prime}$ of the couple.

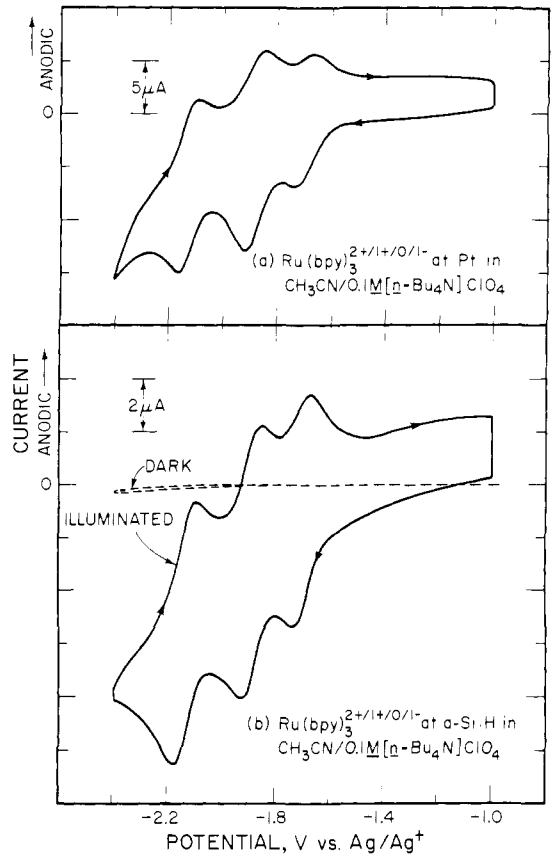

Figure 1. Cyclic voltammetry at (a) Pt and (b) a-Si:H for $Ru(bpy)_3^{2+}$ in CH_3CN/0.1 M [*n*-Bu_4N]ClO_4. The scan rate was 100 mV/s and illumination (632.8 nm) of the a-Si:H was ~40 mW/cm^2.

Consider first the redox behavior of $Ru(2,2'\text{-bpy})_3^{2+}$ illustrated in Figure 1. At a Pt electrode there are three one-electron reductions in dry CH_3CN/0.1 M [*n*-Bu_4N]ClO_4 solution associated with the ~1 mM $Ru(2,2'\text{-bpy})_3^{2+}$ system. In the dark, the a-Si:H electrode results in no significant current over the potential range scanned. Illumination of the a-Si:H with 632.8-nm light, ~40 mW/cm^2, results in cyclic voltammetry waves like those found on Pt, and importantly, the wave positions are in the same position as at Pt. These data show that the illumination effectively makes the a-Si:H a reversible electrode. At ~40 mW/cm^2 illumination the conductivity of the a-Si:H is apparently improved sufficiently to yield good cyclic voltammograms for fast redox couples. Increasing the $Ru(2,2'\text{-bpy})_3^{2+}$ concentration to ~0.15 M results in steady-state current–voltage curves that depend on illumination intensity. At ~40 mW/cm^2 at 632.8 nm, we have been able to observe >10 mA/cm^2 for our typical samples at an electrode potential of −2.0 V vs. SCE in CH_3CN/0.1 M [*n*-Bu_4N]ClO_4/0.15 M $Ru(2,2'\text{-bpy})_3^{2+}$.

The coincidence of the cyclic voltammetry peaks for $Ru(2,2'\text{-bpy})_3^{2+}$ at Pt and at illuminated a-Si:H shows that the a-Si:H gives no photovoltage with respect to the $Ru(2,2'\text{-bpy})^{2+/+/0/-}$ couples. The behavior of *N*,*N*′-dimethyl-4,4′-bipyridinium, MV^{2+}, is quite different at Pt and at illuminated a-Si:H (Figure 2). While both electrodes exhibit cyclic voltammetry waves associated with the $MV^{2+/+/0}$ systems, the wave for the $MV^{2+/+}$ couple at illuminated a-Si:H is considerably more negative than at Pt. The oxidation peak corresponding to the MV^+ to MV^{2+} process at illuminated a-Si:H occurs at an electrode potential ~200 mV more

(12) Dresner, J.; Szostak, D. J.; Goldstein, B. *Appl. Phys. Lett.* **1981**, *38*, 998.

(13) (a) Ellis, A. B.; Kaiser, S. W.; Bolts, J. M.; Wrighton, M. S. *J. Am. Chem. Soc.* **1977**, *99*, 2839. (b) Ginley, D. S.; Butler, M. A. *J. Electrochem. Soc.* **1978**, *125*, 1968. (c) Calabrese, G. S.; Wrighton, M. S. *J. Am. Chem. Soc.* **1981**, *103*, 6273. (d) Tributsch, H. *J. Electrochem. Soc.* **1981**, *125*, 1086. (e) Tributsch, H.; Gerischer, H. *Ibid.* **1978**, *125*, 2085.

(14) (a) Schneemeyer, L. F.; Wrighton, M. S. *J. Am. Chem. Soc.* **1979**, *101*, 6496. (b) Kautek, W.; Gerischer, H. *Ber. Bunsenges. Phys. Chem.* **1980**, *84*, 645. (c) Nakatani, K.; Matsudaira, S.; Tsubomura, H. *J. Electrochem. Soc.* **1978**, *125*, 406.

(15) (a) Frank, S. N.; Bard, A. J. *J. Am. Chem. Soc.* **1975**, *97*, 7427. (b) Kohl, P. A.; Bard, A. J. *Ibid.* **1977**, *99*, 7531. (c) Laser, D.; Bard, A. J. *J. Phys. Chem.* **1976**, *80*, 459.

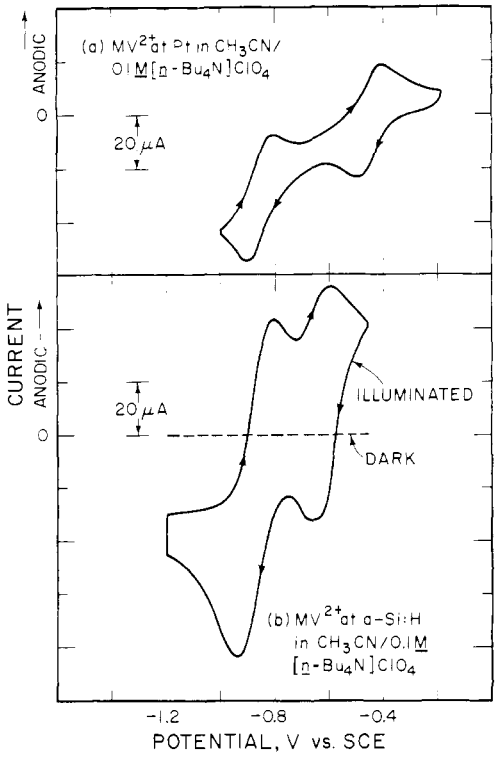

Figure 2. Cyclic voltammetry at (a) Pt and (b) a-Si:H as indicated for MV^{2+} in CH_3CN/0.1 M [n-Bu_4N]ClO_4. The scan rate was 100 mV/s and illumination (632.8 nm) of the a-Si:H was ~40 mW/cm^2.

negative than at Pt. The extent to which the oxidation peak is more negative than at Pt is one measure of E_V and represents the extent to which the light is driving the uphill oxidation process. The $MV^{+/0}$ system exhibits a wave that is nearly coincident with the wave at Pt. Thus, between $E^{\circ\prime}(MV^{2+/+})$ and $E^{\circ\prime}(MV^{+/0})$, uphill photooxidations begin to become a possibility. The potential of ~−0.7 V, the onset of the oxidation of MV^+ to MV^{2+}, can be interpreted as the most positive potential of a redox system that can yield zero field in the a-Si:H. For redox couples that are more negative than −0.7 V, the conduction band of the a-Si:H is apparently contacted, resulting in a sort of ohmic contact to the solution. For redox couples that are more positive than −0.7 V, a field exists across the a-Si:H at redox equilibrium in the dark, analogous to the situation illustrated in Scheme I where the redox couple plays the role of M_2.

The expectation is that the more positive redox couples will give a large photovoltage. Cyclic voltammetry data in Figure 3 illustrate that more positive redox couples than $MV^{2+/+}$ do yield a large E_V, but the dependence is not what would be regarded as ideal. Ideal response would involve a dependence of E_V on E_{redox} as indicated in eq 1, where $E_{CB} \approx -0.7$ V vs. SCE from the data

$$E_{CB} - E_{redox} \approx E_V \qquad (1)$$

above and E_{redox} is situated between E_{VB} and E_{CB}. This relationship indicates that the oxidation of all reduced species should occur at the same potential. However, MV^+, decamethylferrocene, and pentamethylferrocene are oxidized at different electrode potentials. For semiconductor photoanodes, an ideal relationship similar to eq 1 does not always apply because surface states and interface chemistry can result in departures from ideality.[7a] We propose similar difficulties with a-Si:H, including especially problems from photoanodic decomposition of the electrode surface. In fact, for $E^{\circ\prime}$ more positive than ~+0.2 V vs. SCE it is fairly difficult to observe good cyclic voltammetry waves for illuminated a-Si:H in contact with the reduced form of a redox couple. Even for pentamethylferrocene there appears to be problems from photocorrosion current that results in poor output voltage characteristics. Data for the various redox couples at a-Si:H are summarized in Table I. As indicated, data for EtOH and CH_3CN solutions are very similar.

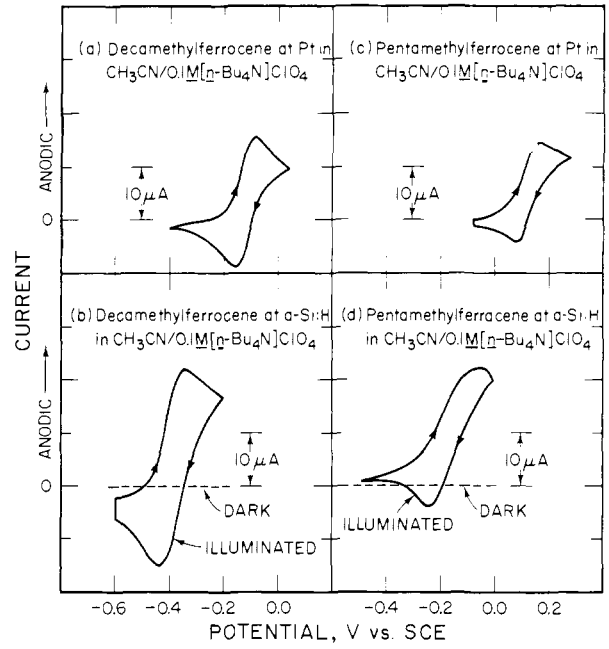

Figure 3. Cyclic voltammetry for Pt and a-Si:H as indicated for pentamethylferrocene and decamethylferrocene in CH_3CN/0.1 M [n-Bu_4N]ClO_4. The scan rate was 100 mV/s and illumination (632.8 nm) of the a-Si:H was ~40 mW/cm^2.

Table I. Cyclic Voltammetry Data for Various Redox Couples at Pt and Illuminated a-Si:H[a]

		Pt		a-Si:H	
redox couple	solvent	E_{PA}	P_{PC}	E_{PA}	E_{PC}
[ferrocene]$^{+/0}$	CH_3CN	+0.46	+0.36	ill defined	
	EtOH	+0.49	+0.41	−0.10	−0.40
[pentamethylferrocene]$^{+/0}$	CH_3CN	+0.16	+0.10	−0.12	−0.24
	EtOH	+0.20	+0.14	−0.20	−0.36
[decamethylferrocene]$^{+/0}$	CH_3CN	−0.08	−0.15	−0.34	−0.40
	EtOH	0.00	−0.07	−0.36	−0.45
$MV^{2+/+}$	CH_3CN	−0.41	−0.48	−0.60	−0.66
$MV^{+/0}$	CH_3CN	−0.82	−0.90	−0.82	−0.90
$Ru(bpy)_3^{2+/+}$	CH_3CN	−1.31	−1.37	−1.31	−1.37
$Ru(bpy)_3^{+/0}$	CH_3CN	−1.51	−1.57	−1.51	−1.57
$Ru(bpy)_3^{0/-}$	CH_3CN	−1.75	−1.81	−1.75	−1.81

[a] Data are from 100 mV/s scans in dry solvent/0.1 M [n-Bu_4N]ClO_4 containing ~1 mM of the redox couple. The a-Si:H electrode was illuminated at 632.8 nm, ~40 mW/cm^2. E_{PA} and E_{PC} refer to anodic and cathodic current peak, respectively. All data were recorded vs. SCE or $Ag/Ag^+ = +0.35$ V vs. SCE. All data are given in V vs. SCE for clarity.

Previous work in this laboratory has established that photoanodes can be protected from photocorrosion by surface modification using (1,1′-ferrocenediyl)dichlorosilane, I, as a derivatizing

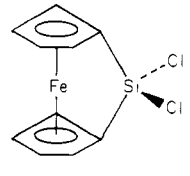

I

reagent.[16] A comparison of the cyclic voltammetry of Pt and illuminated a-Si:H, both derivatized with I, is given in Figure 4. As for solution redox couples, the extent to which the oxidation

(16) (a) Wrighton, M. S.; Austin, R. G.; Bocarsly, A. B.; Bolts, J. M.; Haas, O.; Legg, K. D.; Nadjo, L.; Palazzotto, M. C. *J. Am. Chem. Soc.* **1978**, *100*, 1602. (b) Bolts, J. M.; Bocarsly, A. B.; Palazzotto, M. C.; Walton, E. G.; Lewis, N. S.; Wrighton, M. S. *Ibid.* **1979**, *101*, 1378. (c) Bocarsly, A. B.; Walton, E. G.; Wrighton, M. S. *Ibid.* **1980**, *102*, 3390. (d) Bocarsly, A. B.; Walton, E. G.; Bradley, M. G.; Wrighton, M. S. *J. Electroanal. Chem.* **1979**, *100*, 283.

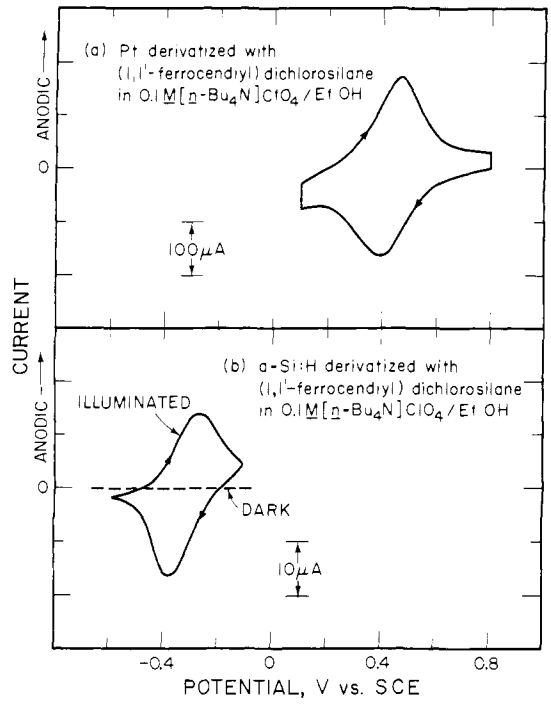

Figure 4. Cyclic voltammetry for (a) Pt and (b) a-Si:H derivatized with (1,1'-ferrocenediyl)dichlorosilane in EtOH, 0.1 M $[n\text{-}Bu_4N]ClO_4$. The scan rate was 100 mV/s and illumination (632.8 nm) of the a-Si:H was ~40 mW/cm^2.

Table II. Output Parameters for an a-Si:H-Based Photoelectrochemical Cell Employing the Ferricenium/Ferrocene Redox Couple[a]

input, mW/cm^2	Φ_e at E_{redox}[b]	E_V-(max)[c]	η_{max}, % (E_V at η_{max})[d]	fill factor[e]
0.7	0.23	670	4.5 (460)	0.49
1.4	0.23	690	4.1 (460)	0.47
2.8	0.23	720	3.7 (460)	0.44
4.2	0.22	730	3.5 (460)	0.44
5.7	0.21	740	3.3 (460)	0.42
9.3	0.19	750	3.1 (460)	0.43

[a] Data are associated with the steady-state photocurrent-voltage curves given in Figure 5 for a ferricenium/ferrocene/EtOH 0.1 M $[n\text{-}Bu_4N]ClO_4$ solution illuminated with a 632.8-nm light source. [b] Quantum yield for electron flow at $E_f = E_{redox} = +0.38$ V vs. SCE. [c] Open-circuit photovoltage. [d] Maximum efficiency for conversion of 632.8-nm light to electricity and the output voltage at the maximum power point. [e] Fill factor is (photocurrent at $\eta_{max} \times E_V$ at η_{max})/(photocurrent at $E_{redox} \times E_V$(max)).

wave is more negative for the illuminated electrode is a measure of E_V. The data in Figure 4 indicate an E_V of ~750 mV, significantly larger than found for the solution redox couples (Table I and Figures 1-3). It is not certain that the ability to observe E_V = 750 mV is due to the fact that the derivatized surface is more durable. What is important is that the results shown in Figure 4 indicate that E_V can be fairly large. The E_V for the a-Si:H is somewhat larger than that routinely observed from single-crystal n-type Si (E_g = 1.1 eV) derivatized with I under the same conditions.[16] However, even for a-Si:H derivatized with I we do not find as large a value of E_V as would be expected based on eq 1.

c. Conversion of Light to Electricity Using a-Si:H-Based Cells. High concentrations of fast, one-electron reductants are useful in suppressing the photocorrosion of semiconducting photoanodes. We find that EtOH/0.1 M $[n\text{-}Bu_4N]ClO_4$ electrolyte solutions containing high concentrations of ferrocene do protect a-Si:H from photocorrosion. Representative steady-state photocurrent–voltage curves for an a-Si:H-based cell with an E_{redox}(ferricenium/ferrocene) = +0.38 V vs. SCE are shown in Figure 5, and a summary

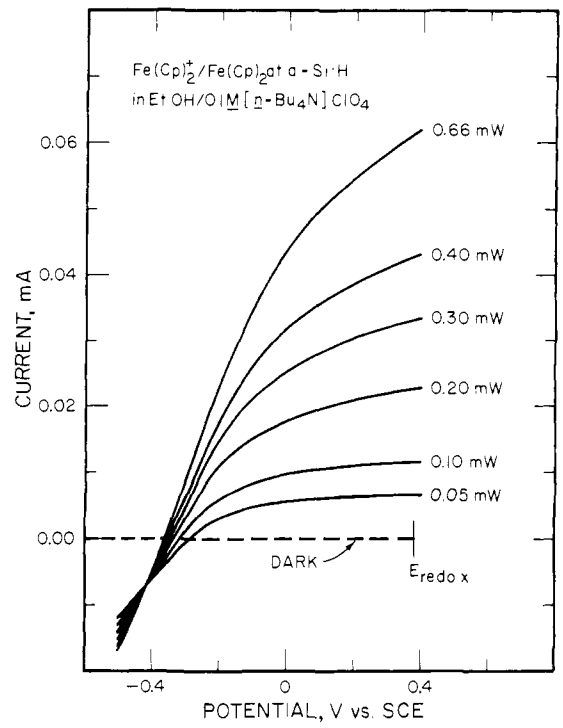

Figure 5. Representative steady-state current–voltage curves for an ~0.07 cm^2 a-Si:H electrode in EtOH containing 0.075 M $Fe(Cp)_2$, ~1 mM $Fe(Cp)_2^+$, and 0.1 M $[n\text{-}Bu_4N]ClO_4$. Incident 632.8-nm optical power is given in mW. The redox potential of the solution was +0.38 V vs. SCE.

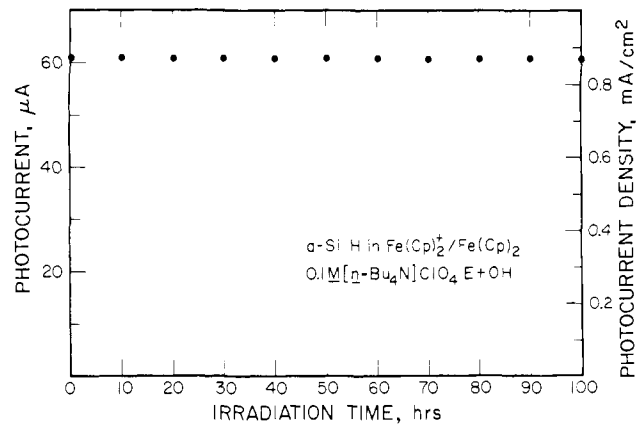

Figure 6. A plot of photocurrent against time for a ~0.07 cm^2 a-Si:H electrode potentiostatted at 0.0 V vs. SCE and irradiated with 632.8-nm light (~10 mW/cm^2). The run was performed in dry Ar-purged EtOH containing 0.075 M $Fe(Cp)_2$, ~1 mM $Fe(Cp)_2^+$, and 0.1 M $[n\text{-}Bu_4N]ClO_4$, giving an E_{redox} of +0.38 V vs. SCE. The efficiency for conversion of light to electricity is (power out/power in) × 100% = 3.3%.

of the output parameters is given in Table II. The open-circuit photovoltage, E_V(max), from the steady-state curves is the equivalent of the photovoltage measured by cyclic voltammetry. However, at the high concentration (~0.07 M) of ferrocene there is not detectable photocorrosion and a good photovoltage is attainable (Table II). Figure 6 illustrates that a photocurrent density of ~0.9 mA/cm^2 can be sustained for >100 h without variation for the ferricenium/ferrocene redox couple system for a light intensity of ~10 mW/cm^2. Subsequent to the experiment summarized by Figure 6, the 632.8-nm input light intensity was raised to ~40 mW/cm^2 and the photocurrent increased and remained constant, within 2%, for the succeeding 48 h. Thus, the a-Si:H appears to be durable even at an input intensity similar to that from the visible portion of the solar spectrum. It appears that electrical output can be sustained indefinitely under the conditions employed, consistent with earlier findings from this laboratory

for single-crystal n-type Si-based cells.

The overall efficiency for an a-Si:H cell (Table II) is slightly better than we have typically found for a single-crystal n-type Si-based cell.[16b,17] The output photovoltage is higher, but the quantum yield is lower, for the a-Si:H. The low observed quantum yield is partly due to the fact that the values given are uncorrected for reflection losses of ~30% at 632.8 nm. Another possible loss is the relatively low absorbance of incident 632.8-nm light. The fact that current flows at all is due to the fact that carriers are created throughout the thickness of the film, but not all carriers survive to be collected at the contact and electrolyte. The absorptivity[3] at 632.8 nm is $\sim 10^4$ cm^{-1}, suggesting that a significant number of carriers are generated at a depth of >0.5 μm from the surface. Some photogenerated holes beyond this depth may not arrive at the electrolyte, despite the field driving them toward the electrolyte. Shorter wavelength light is absorbed more strongly such that carriers can be created closer to the surface. However, such will not lead to sufficient carriers deep below the surface to result in a current. Consequently, 454.4- or 514.5-nm light from an Ar ion laser gives lower observed quantum yields than does 632.8-nm light at the same intensity in photons/(cm^2 s). When white light (from an incandescent source, 200-W tungsten lamp) is used to create carriers throughout the material, the observed quantum yield for additional light at 514.5 nm can be determined to be somewhat greater than from additional 632.8-nm light. White light irradiation to give the same current density at E_{redox} as the 632.8-nm light in Figure 5 does not lead to improved fill factors that might be expected for more uniform carrier distribution. The improvements possible with white light alone, or the conversion efficiency from 632.8 or 514.5 nm monochromatic light when the surface is simultaneously illuminated with white light, are not dramatic. Another source of inefficiency may be due to the use of a relatively thick a-Si:H layer. Despite the fact that the material is nearly intrinsic, the low carrier concentration in the 3.9-μm thickness likely means that the field across the material is much stronger near the surface. The point is that the representations in Schemes I–IV showing uniform fields across the photoconductor do not strictly apply to the samples used here. Thinner samples may give improved quantum efficiencies and fill factors since the field could extend across the entire material.

(17) Legg, K. D.; Ellis, A. B.; Bolts, J. M.; Wrighton, M. S. *Proc. Natl. Acad. Sci. U.S.A.* **1977**, *74*, 4116.

Summary

Intrinsic a-Si:H can be used as an electrode in electrochemical cells when ≥1.7-eV light is used to create a significant carrier density throughout the material. For redox couples having $E^{\circ\prime}$ more negative than ~−0.7 V vs. SCE, the electrochemistry occurs at potentials expected for a reversible electrode. For $E^{\circ\prime}$ more positive than −0.7 V vs. SCE, the oxidation of the reduced form of the couple can be effected in an uphill sense using the light as the driving force. Nonideal interface properties appear to limit the maximum attainable photovoltage to ~750 mV. Importantly, the a-Si:H photoelectrode can be durable when the proper solvent/electrolyte/redox couple combination is used. Sustained conversion (>100 h) of monochromatic 632.8-nm light (10 mW/cm^2) with an efficiency of ~3.3% has been demonstrated.

Acknowledgment. We thank the U.S. Department of Energy, Office of Basic Energy Sciences, Division of Chemical Sciences, and the Dow Chemical Company for support of the work at M.I.T. We thank Professor William Paul and Garrett Moddel of the Division of Applied Sciences, Harvard University, for useful discussions. M.S.L. acknowledges support from the Division of Applied Sciences, Harvard University, for graduate research performed at M.I.T.

Registry No. $Fe(Cp)_2$, 102-54-5; $Fe(Cp)_2^+$, 12125-80-3; [pentamethylferrocene]$^+$, 81064-27-9; pentamethylferrocene, 63074-30-6; [decamethylferrocene]$^+$, 54182-41-1; decamethylferrocene, 12126-50-0; MV^{2+}, 4685-14-7; MV^+, 25239-55-8; MV, 25128-26-1; $Ru(bpy)_3^{2+}$, 15158-62-0; $Ru(bpy)_3^+$, 56977-24-3; $Ru(bpy)_3$, 74391-32-5; $Ru(bpy)_3^-$, 56977-23-2; Pt, 7440-06-4; Si, 7440-21-3; (1,1′-ferrocenediyl)dichlorosilane, 66083-73-6; stainless steel, 12597-68-1.

Synthesis and X-ray Structure of *cis*-Tetracarbonyl[(*Z*)-(η^2-allylamino)(*p*-tolyl)carbene]-tungsten(0), a Stable Metal–Carbene–Alkene Complex

Charles P. Casey,* Alan J. Shusterman, Nicholas W. Vollendorf, and Kenneth J. Haller

Contribution from the Department of Chemistry, University of Wisconsin, Madison, Wisconsin 53706. *Received July 31, 1981*

Abstract: Allylamine and 1-amino-3-butene react with $(CO)_5WC(OCH_3)C_6H_4$-*p*-CH_3 to produce $(CO)_5WC(NHCH_2CH{=}CH_2)C_6H_4$-*p*-$CH_3$ ((*Z*)-**3** and (*E*)-**3**) and $(CO)_5WC(NHCH_2CH_2CH{=}CH_2)C_6H_4$-*p*-$CH_3$ ((*Z*)-**4** and (*E*)-**4**) as mixtures of isomers about the carbene carbon–nitrogen partial double bond. The alkene units in **3** and **4** are not coordinated to tungsten. Thermolysis or photolysis of a mixture of (*Z*)-**3** and (*E*)-**3** leads to formation of $(CO)_4W(NHCH_2CH{=}CH_2)C_6H_4$-*p*-$CH_3$ (**5**), a stable tungsten–carbene–alkene complex. The X-ray crystal structure of **5** shows a perpendicular arrangement of the alkene and carbene ligands. Crystal data for **5**: space group $P2_1/n$; $Z = 4$, $a = 7.989$ (1) Å, $b = 18.374$ (2) Å, $c = 10.875$ (1) Å, $\beta = 105.54$ (1)°; $V = 1538$ Å^3; $R = 0.037$ and $R_w = 0.047$ for the 2851 reflections with $F_o > 3\sigma(F_o)$. Attempts to prepare a tungsten–carbene–alkene complex with a larger chelate ring from **4** led to double-bond isomerization and isolation of $(CO)_4W[NHCH_2CH{=}CHCH_3]C_6H_4$-*p*-$CH_3$ (**11**).

Metal–alkene–carbene complexes and metallacyclobutanes have been proposed as key intermediates in several metal-catalyzed reactions. In the olefin metathesis reaction, the observed nonpairwise exchange of alkylidene groups is thought to occur via the equilibration of metal–alkene–carbene complexes and metallacyclobutanes.[1] The metal-catalyzed cyclopropanation of alkenes is proposed to occur by reductive elimination of the product cyclopropane from a metallacyclobutane intermediate.[2] In ad-

(1) Grubbs, R. H. *Prog. Inorg. Chem.* **1978**, *24*, 1–50. Katz, T. J. *Adv. Organomet. Chem.* **1977**, *16*, 283–317. Calderon, N.; Lawrence, J. P.; Ofstead, E. A. *Ibid.* **1979**, *17*, 449–492.

0002-7863/82/1504-2417$01.25/0